Journal Pre-proof

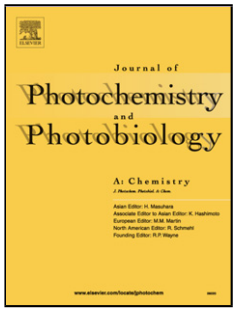

A diarylethene derived Fe^{3+} fluorescent chemosensor and its application in wastewater analysis

Yongjie Li, Wenhao Pan, Chunhong Zheng, Shouzhi Pu

PII: S1010-6030(19)31733-2

DOI: https://doi.org/10.1016/j.jphotochem.2019.112282

Reference: JPC 112282

To appear in: *Journal of Photochemistry & Photobiology, A: Chemistry*

Received Date: 9 October 2019

Revised Date: 27 November 2019

Accepted Date: 2 December 2019

Please cite this article as: Li Y, Pan W, Zheng C, Pu S, A diarylethene derived Fe^{3+} fluorescent chemosensor and its application in wastewater analysis, *Journal of Photochemistry and amp; Photobiology, A: Chemistry* (2019), doi: https://doi.org/10.1016/j.jphotochem.2019.112282

A diarylethene derived Fe^{3+} fluorescent chemosensor and its application in wastewater analysis

Yongjie Li, Wenhao Pan, Chunhong Zheng* and Shouzhi Pu*

Jiangxi Key Laboratory of Organic Chemistry, Jiangxi Science and Technology Normal University, Nanchang 330013, PR China

*Corresponding author: ezirobot@163.com, (C. Zheng), pushouzhi@tsinghua.org.cn (S. Pu), Tel/Fax.: +86-791-83831996.

Graphical abstract

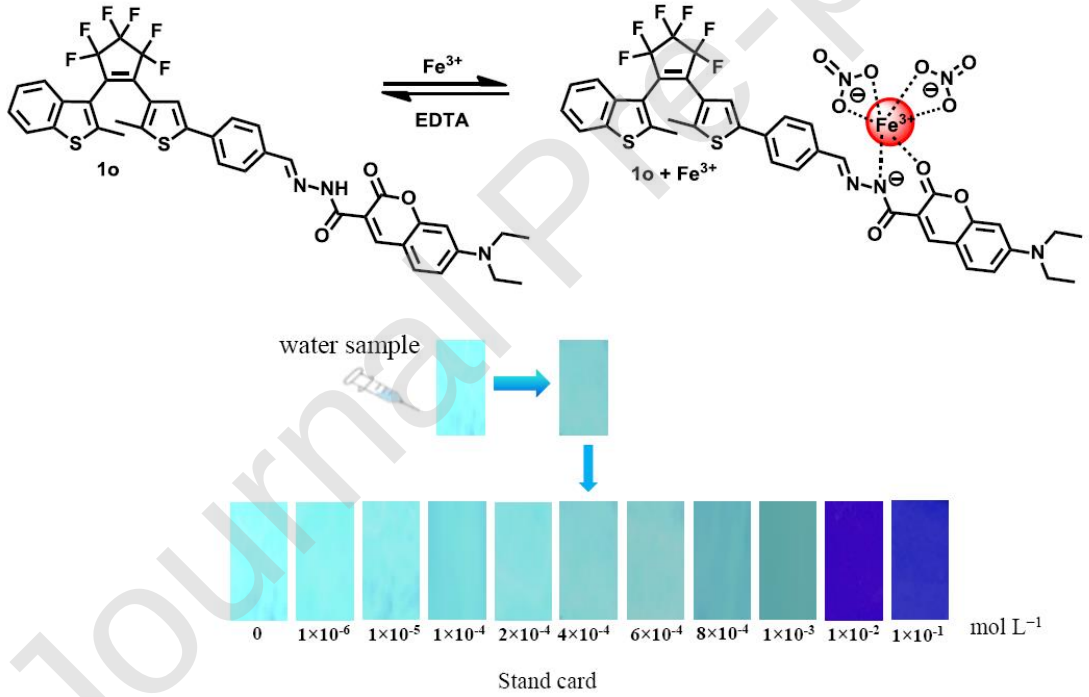

A diarylethylene derivative containing an acylhydrazone Schiff base moiety was designed and synthesized, and its sensing for the Fe^{3+} ion was studied. The fluorimetric test paper for Fe^{3+} were prepared and could be used to measure Fe^{3+} concentration in wastepaper by comparison with the standard card.

Highlights

- A diarylethylene derivative containing an acylhydrazone Schiff base moiety was designed and synthesized.
- The derivative showed a selective and fluorescence changes upon addition of Fe^{3+}.
- The sensing for Fe^{3+} was well demonstrated by the standard card, which can be evaluated Fe^{3+} concentrations directly and quickly.

Abstract

A diarylethylene derivative containing an acylhydrazone Schiff base moiety was designed and synthesized. Upon alternative irradiation with UV and visible lights, the compound showed distinct fluorescence switching properties based on fluorescence resonance energy transfer mechanism. On the other hand, the fluorescence can be efficiently quenched by 69 fold in the presence of Fe^{3+} ion in methanol. As a Fe^{3+} fluorescent chemosensor, the sensing mechanism, the influence of pH on sensing properties, and the practical application were also studied. In the complex, the breaking of the intramolecular H-bonding between the –CO=NH– proton and the oxygen at the C=O of lactone, the weaking of electrons transfer, and the paramagnetic nature of Fe^{3+} induced a consequent decrease fluorescence. The compound was found to be stable in a wide range of pH and a highly efficient Fe^{3+} ion quencher with a detection limit of 4.6×10^{-6} mol L^{-1}. Moreover, the fluorescent detection of Fe^{3+} was demonstrated by filter paper strips. A series of test papers with different Fe^{3+} concentrations were prepared and used as the standard card. The analytical application of measuring Fe^{3+} concentration in wastewater samples were evaluated by comparison with the standard card directly and quickly.

Keywords: Photochromism; Diarylethene; Acylhydrazone Schiff base; Fluorescent chemosensor; Fe^{3+} ion sensing; Test strip

1. Introduction

Ion ion (Fe^{3+}), as one of the biologically important metal ions, plays an essential role in synthesizing a series of enzymes involved in oxygen uptake, oxygen metabolism, and electron transfer [1,2]. Imbalanced Fe^{3+} levels seriously affect the normal activities of organisms [3]. High concentrations in the body will lead to the imbalance between oxidation and antioxidation which damage DNA and induced mutation [4−6]. And deficiency will cause anaemia and related discrepancies such as impaired cognitive function, lethargy, low immunity [7]. Fe^{3+} can also cause potential health hazards through the food chain due to its migration and enrichment in the environment in environment water system [8]. Therefore, the development of reliable and sensitive chemosensor for the monitoring of the Fe^{3+} is highly desirable. In recent decades, a rapid advancement in analytical technology for metal ion is optical chemosensors. Among them, fluorescence sensors have attracted much attention due to its low detection levels, high selectivity and sensitivity and ease of operation [9]. So far, a large variety of fluorescence sensors have been designed based on various identification mechanisms, such as PET [10], FRET [11], ICT [12,13], and ESIPT [14] etc. Although most of them showed highly selective recognition of a particular ion and meet the specific recognition function, there are very few fluorescent sensors for Fe^{3+} ions. Thus, a highly selective fluorescent chemosensor for Fe^{3+} is an immediate required.

Diarylethene, as one of the photochromic molecules, has two different molecular forms. They are characterized by a reversible transformation between the open-ring and closed-ring forms with distinct absorption spectra upon alternative irradiation with UV and visible light [15–18]. Most diarylethene molecules are not appreciably fluorescent on their own, but combining them with a fluorophore has been used to modulate the fluorescence [19,20]. Coumarin group was frequently chosen as the fluorophore due to its excellent spectroscopic properties, light stability and less toxicity [21]. When a suitable receptor was attached to the fluorophore, a desired chemosensor would be constructed by fluorescence change mechanism [22]. Both N and O atoms are frequently the donor atoms, which readily combine with transition metal cations such as Cu^{2+} [23], Co^{2+} [24], Fe^{3+} [25], Zn^{2+} [26]. Usually, diarylethenes-based chemosensors were conducted by combining a diarylethene core and an appending functionalized fluorophore by different reaction such as aldimine condensation [27], Click chemistry [28], Willimson chemistry [29], Heck chemistry [30],

etc. Among them, aldimine condensation is the most commonly strategy due to its easily synthesize, high yields. Until now, despite of all these efforts being devoted to the diarylethene-based chemosensors containing a salicylidene Schiff base group [31], seldom fluorescent and colorimetric sensors for Fe^{3+} have been achieved.

Herein, a diarylethene derivative (**1o)** containing an acylhydrazone Schiff base moiety was designed and synthesized. Experiments showed that **1o** showed evident absorption spectral and emission spectral changes upon alternative irradiation with UV and visible lights. More importantly, Fe^{3+} could selectively and sensitively control the fluorescence of **1o**. The structure, the isomer transformation in the presence of light and Fe^{3+} are shown in Scheme 1.

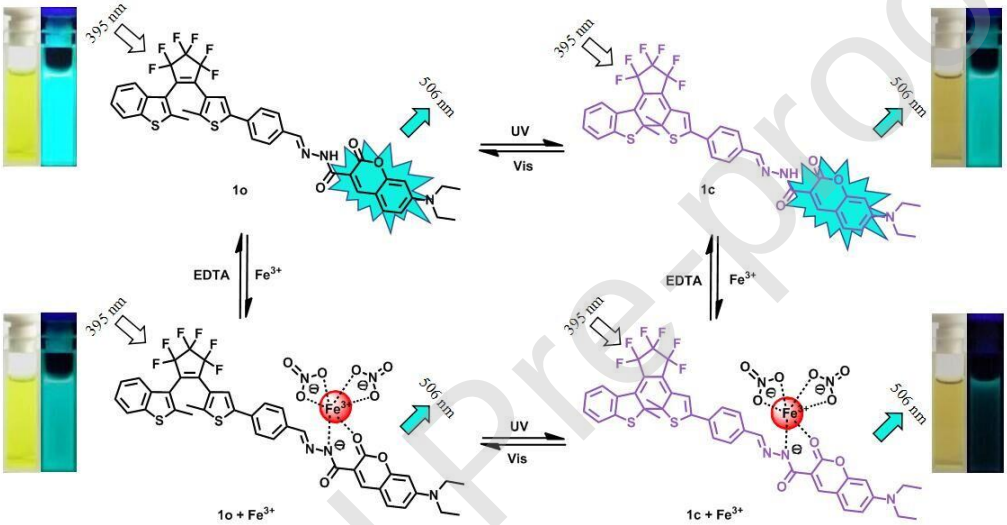

Scheme 1. The structure, photochromism of **1o** and sensing for Fe^{3+}.

2. Experimental

2.1 General methods

Chemical reagents were purchased from either Alfa or TCI and can be used without further purification. Solvents were obtained from Beijing Chemical Plant. Anhydrous solvents were of spectroscopic quality and purified by distillation prior to use. All solution-phase reactions were carried out under dry argon atmosphere. Reactions were monitored by analytical thin-layer chromatography on plates coated with 0.25 mm silica gel 60 F254 (Qingdao Haiyang Chemical). Melting points were measured with a WRS-1B melting point apparatus. Infrared spectra were recorded on a Bruker Vertex–70 spectrometer. The fluorescence quantum yields were measured by Perkineimer lambea 750 UV/vis. NMR spectra were obtained on a Bruker AV–400 spectrometer

with tetramethyl silane (TMS) as internal reference and $CDCl_3$ as solvent. Absorption spectra were obtained with an Agilent 8454 UV/vis spectrometer. Fluorescence spectra were studied in a Hitachi F-4600 fluorescence spectrophotometer. Photoirradiation was carried out with an SHG–200 UV lamp, a CX–21 ultraviolet fluorescence analysis cabinet, and a BMH–250 visible lamp. Light of appropriate wavelengths was isolated by light filters. The measurements of pH values were recorded on a PHS–3C pH meter (Shanghai, China).The metal ions were prepared by dissolving their their respective salts (0.20 mmol) in distilled water (2 mL). Aqueous solutions of Ag^+, Ba^{2+}, Cu^{2+}, Zn^{2+}, Cd^{2+}, Mn^{2+}, Fe^{3+}, Pb^{2+}, Ca^{2+}, Co^{2+}, Cr^{3+}, Ni^{2+}, Mg^{2+}, Sn^{2+}, and Al^{3+} were prepared using their corresponding nitrates, and K^+, Hg^{2+} were prepared using their corresponding chlorides.

2.2. Synthesis

Compound **3** was prepared by reacting **2** with $N_2H_4{\cdot}H_2O$ in methanol, which was further condensated with **4** [32] to yield compound **1o**. The synthesis of **1o** was illustrated as shown in Scheme 2.

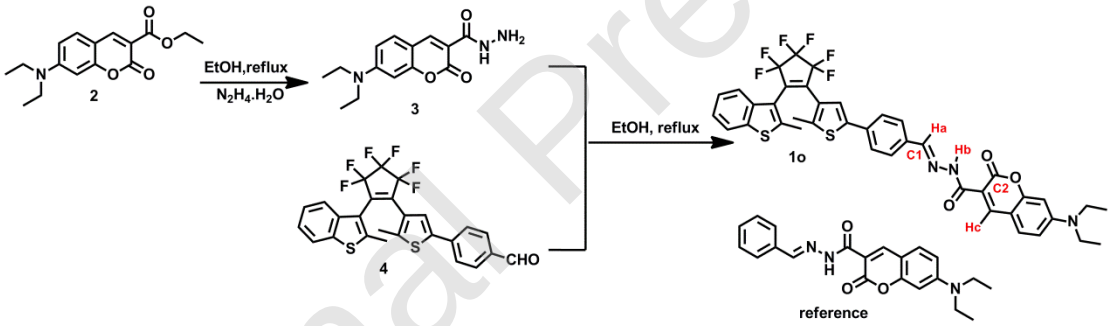

Scheme2. The synthesis route of **1o**.

2.2.1 Synthesis of 7-diethylamino-3-hydrazide-coumarin (**3**)

According to the previous procedure [33], to a stirred solution of ethyl 7-(diethylamino)coumarin-3-carboxylate (1.0 g, 3.5 mmol) in 20 ml absolute ethanol, hydrazine hydrate (1 mL, 20.4 mmol) was injected at room temperature, the mixture was refluxed for overnight. The system was cooled down to room temperature, and subsequently filtered off and washed with cold ethanol. The produce was recrystallized from ethanol to give yellow solid at a yield of 82%. ^{1}H NMR (400 MHz, $CDCl_3$): δ (ppm) 1.24 (t, 6H, $–CH_3$, J = 8.0 Hz), 3.46 (m, 4H, $–CH_2$, J = 8.0 Hz), 4.16 (s, 2H, $–NH_2$), 6.48 (s, 1H, phenyl-H), 6.65 (d, 1H, phenyl–H, J = 8.0 Hz),

7.43 (d, 1H, phenyl–H, J = 8.0 Hz), 8.67 (s, 1H, =C–H), 9.73 (s, 1H, –NH); ^{13}C NMR ($CDCl_3$, 100 MHz), δ (ppm): 11.41, 44.09, 95.62, 107.25, 108.15, 109.02, 130.12, 146.98, 151.69, 156.62, 161.07, 162.84.

2.2.2 Synthesis of 1-(2-methyl-3-benzothiophenyl)-2-{2-methyl-5-[4-(7-diethylamino coumarinhydrazide)-phenyl]-3-thienyl}perfluorocyclopentene (**1o**)

To a stirred solution of compound **4** (0.105 g, 0.2 mmol) in 10 mL ethanol, compound **3** (0.041g, 0.2 mmol) was added. The mixture was refluxed for 6 h and no compound **4** was detected by thin-layer chromatography silica gel plate. A yellow solid was obtained with 85% yield by vacuum evaporating the solvent. M.p. 452–453 K. ^{1}H NMR (400 MHz, $CDCl_3$): δ (ppm) 1.26 (t, 6H, –CH_3, J = 8.0 Hz), 1.96 (s, 3H, –CH_3), 2.31 (s, 3H, –CH_3), 3.48 (m, 4H, –CH_2, J = 8.0 Hz), 6.53 (s, 1H, phenyl–H), 6.69 (d, 1H, phenyl–H, J = 8.0 Hz), 7.22 (s, 1H, thiophene–H), 7.31–7.34 (t, 1H, phenyl–H, J = 6.0 Hz), 7.37–7.38 (d, 1H, phenyl–H, J = 4.0 Hz), 7.44 (d, 2H, phenyl–H, J = 8.0 Hz), 7.49 (d, 1H, phenyl–H, J = 8.0 Hz), 7.58 (d, 1H, phenyl–H, J = 7.8 Hz), 7.74–7.76 (d, 1H, phenyl–H, J = 8.0 Hz), 7.77 (s, 1H, phenyl–H), 7.79 (s, 1H, phenyl–H), 8.17 (s, 1H, H_c), 8.86 (s, 1H, H_b), 11.92 (s, 1H, Ha; ^{13}C NMR ($CDCl_3$, 100 MHz), δ (ppm): 11.41, 13.84, 17.42, 19.29, 44.19, 57.47, 95.60, 107.63, 107.95, 109.30, 119.26, 121.08, 122.24, 123.53, 123.97, 124.35, 124.49, 127.40, 130.44, 132.28, 133.91, 137.22, 140.05, 141.34, 141.49, 146.60, 148.21, 152.00, 156.84, 158.89,161.81; IR (ν, KBr, cm^{-1}): 3058 (N–H), 1697 (C=O), 1617 (C=N), 1385 (C–O–C); LRMS ($ESI^{-)}$ m / z: $[M – H]^–$, calcd, 778.2; found, 778.0.

3. Results and discussion

3.1 Photochromism properties of **1o**

The photochromic behavior of **1o** with stimulation UV and visible lights in methanol (1.0×10^{-5} mol L^{-1}) at room temperature was studied. As shown in Fig 1A, the absorption spectrum of **1o** in methanol exhibits absorption bands at 226, 262, 337 and 440 nm. The maximum absorption at 440 nm is due to the 7-N,N′-diethylamine coumarin-3-hydrazide-1-benzaldehyde Schiff base (reference) (Fig. S1), which has a maximum absorption at 433 nm. The photochromic core decreased the electron-donating ability of the shiff base moiety within **1o**, which enhanced the degree of intramolecular charge transfer (ICT).Thus, a 7 nm red-shift was observed. Consistently,

the red-shifted behavior (2 nm) was also observed in the fluorescence emission spectrum of **1o** (Fig. S2). Upon irradiation with 297 nm light, the peaks at 226, 262, 337, and 440 nm were little changed due to these absorption peaks overlapped that of coumarin derivative. The absorption coefficient of 7-N,N'-diethylamine coumarin-3-hydrazide-1-benzaldehyde Schiff base is similar to that of **1o**, indicating that most of the absorption of **1o** at 440 nm is due to the 7-N,N'-diethylamine coumarin-3-hydrazide-1-benzaldehyde Schiff base. Little of the absorbed photons by **1o** can be used for the photocyclization reaction. A new absorption peak at 554 nm appeared due to the formation of the closed-ring isomer **1c** accompanied by an immediate color change from yellow to dark yellow. When the photostationary state was arrived, three clear isosbestic points were observed at 269, 323 and 360 nm, indicating a two-component photochromic reaction process [34]. Upon irradiation with visible light (> 510 nm), the dark yellow color faded and the absorption spectrum returned to the initial state of **1o**.

The presence of a 7–N$(C_2H_5)_2$ group and 3–CONHN=CH–benzene group at the coumarin fluorophore in **1o** induced the transfer of electrons within the molecule, like a push-pull system [35]. Thus, compound **1o** alone displays a strong and single fluorescence emission band at 506 nm with a fluorescence quantum yield (Φ = 0.13), when excited at 395 nm. The intramolecular H-bonding stabilization between the –CO=NH– proton and the oxygen at the C=O of lactone also enhanced the fluorescence [36]. As most of the reported diarylethenes [37], **1o** exhibited a relatively strong fluorescence switch, as shown in Fig 1B. Upon irradiation with 297 nm light, the emission intensity gradually decreased. When the photostationary state was arrived, the emission intensity of **1o** was quenched to ca. 29.64%. This was ascribed to the formation of the closed-ring isomer of **1c**, accompanied by the fluorescence resonance energy transfer (FRET) [38]. The emission band of the 7-diethylamino coumarinhydrazide unit **3** was 494 nm (430–650 nm), and the absorption peak of the colosed-ring isomer of the photochromic core **4** was 548 nm (450–670 nm) (Fig. S3). The emission band of **3** well overlaps with the absorption wave range of the colosed-ring isomer of diarylethene **4,** which is helpful for the FRET. Thus, upon irradiation with 297 nm light, the energy was transferred from the excited 7-diethylamino coumarinhydrazide unit to the photochromic core **4**, accompained by the fluorescence quenching. Reversely, the fluorescence of **1o** could be restored upon irradiation with appropriate visible light (λ > 510 nm).

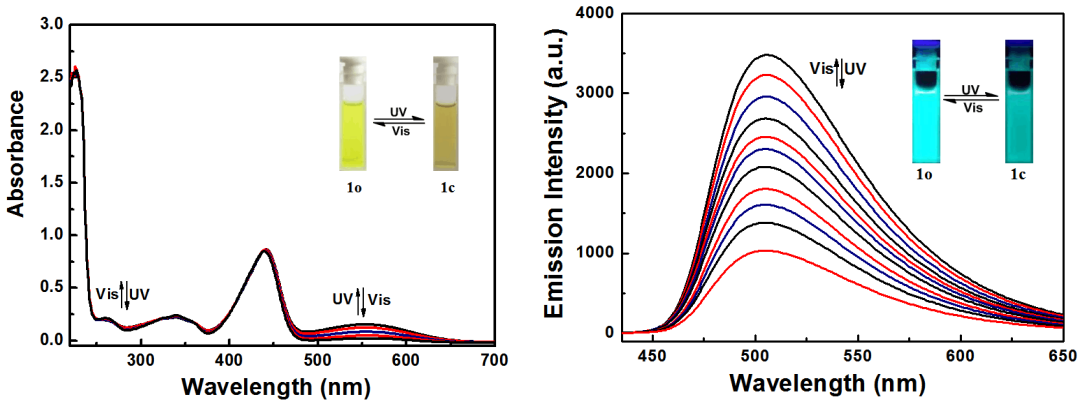

(A) (B)

Fig. 1. (A) Absorption spectral and color changes of **1o** upon alternating irradiation with UV–vis light in methanol (1.0×10^{-5} mol L^{-1}); and (B) Fluorescence spectral and color changes of **1o** upon alternating irradiation with UV–vis light in methanol (1.0×10^{-5} mol L^{-1}).

3.2 Detection of Fe^{3+} in methanol

The metal ions recognition of **1o** was studied by fluorescence spectroscopy. As shown in Fig. 2A, addition of 10 equiv. of metal ions (Fe^{3+}, Cr^{3+}, Mn^{2+}, Co^{2+}, Ni^{2+}, Cu^{2+}, Zn^{2+}, Cd^{2+}, Hg^{2+}, Pb^{2+}, K^{+}, Mg^{2+}, Ca^{2+}, Ba^{2+}, Sn^{2+} and Al^{3+}) to **1o** in methanol (1.0×10^{-5} mol L^{-1}) induced major quenching of fluorescence intensity for Fe^{3+} due to the formation of **1o**–Fe^{3+} complex. Compared with the free **1o**, the fluorescence quantum yield was decreased by 69 fold ($\Phi_{Fe} = 0.04$, $\Phi_{Fe} / \Phi_0 = 69$). Moreover, for the co-existence of Fe^{3+} ion and other ions, the fluorescence intensity was similar to that in the presence of only Fe^{3+}, as shown in Fig. 3. The result indicated a highly selective response of **1o** for Fe^{3+} as compared to the other metal ions.

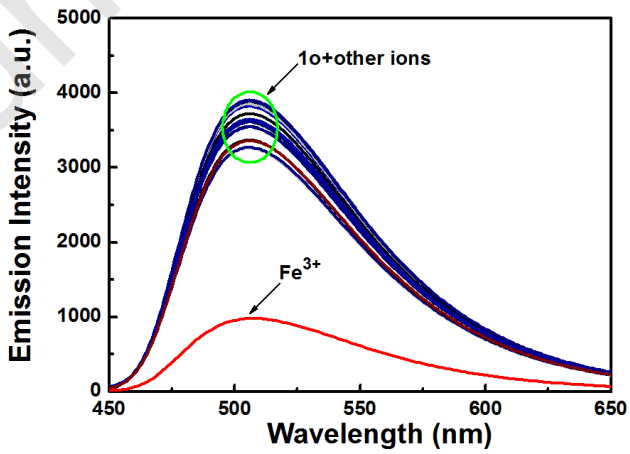

(A)

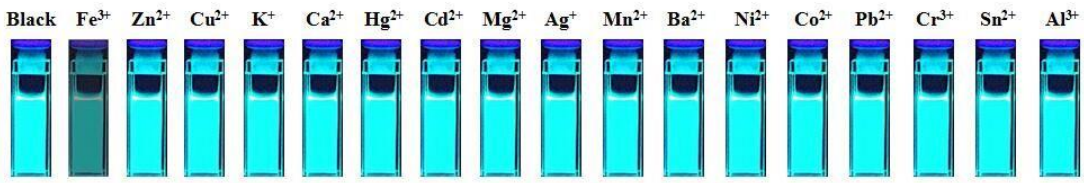

(B)

Fig. 2. (A) Fluorescence spectral of **1o** in methanol (1.0×10^{-5} mol L^{-1}) upon addition of 10 equiv. of various metal ions; and (B) Fluorescent photos of **1o** with various metal ions.

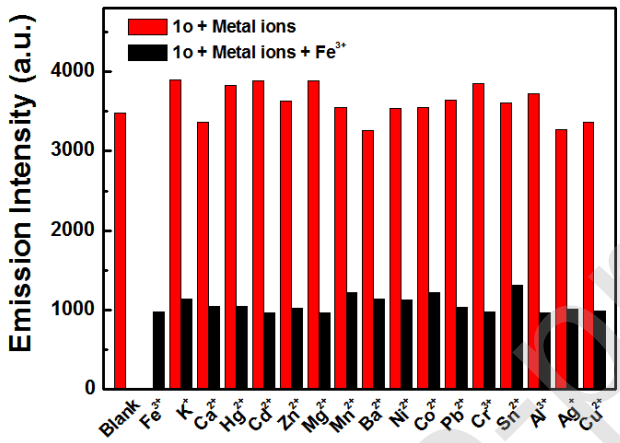

Fig. 3. Responses of **1o** in methanol (1.0×10^{-5} mol L^{-1}) to various anions. Red bars represent the addition of 10 equiv. various anions to the solution of **1o**. Black bars represent the addition of 10 equiv. Fe^{3+} to the above solution, respectively.

The changes in the e emission intensity of **1o** with the different Fe^{3+} concentrations at room temperature was shown in Fig. 4A. With the addition of changeable amounts of Fe^{3+}, the emission intensity at 506 nm gradually decreased. When 11 equiv. of Fe^{3+} was added, **1o** opened a nonradiative deactivation channel induced by paramagnetism with an unfilled d shell. The binding of Fe^{3+} and **1o** initiated a charge transfer, which inhibited the electron transfer with **1o**, causing 28% fluorescence quenching [39].. The interaction between **1o** and Fe^{3+} could occur at C=O of lactone, and –NH, which could be identified as binding to transition and post transition metals [40]. Job's plot was carried out to determine the binding stoichiometry of **1o** with Fe^{3+}. As shown in Fig. 4B, the intensity of the system with themolar ratio of Fe^{3+} for a series of solutions, in which the total concentration of **1o** and Fe^{3+} was kept constant. Feature point appeared at 0.5 on the abscissa, indicating a 1 : 1 stoichiometry between **1o** and Fe^{3+}. Using the fluorescence titration data, the 1 : 1 stoichiometry between **1o** and Fe^{3+} was further confirmed by the Benesi–Hildebrand

equation, as shown in Fig. 4C. The association constant (K_a) was calculated to be 1.49×10^5 mol^{-1} L by using the Benesi–Hildebrand equation. The detection limit of Fe^{3+} was obtained by plotting a graph between the relative emission intensity at 506 nm as a function of the Fe^{3+} constrations. Based on 3σ / S, the limit of detection of **1o** for Fe^{3+} was 4.6×10^{-6} mol L^{-1} (Fig. 4D). Compared with the recently reported Fe^{3+} sensors (Table 1), **1o** has relatively high association constant and low limit of detection. Moreover, the emission intensity of **1o**–Fe^{3+} could completely returned to that orginal state **1o** upon adding of EDTA, which demonstrated that **1o** sensed Fe^{3+} reversibly. The coordination-dissociation cycles can be repeated four times (Fig. S4).

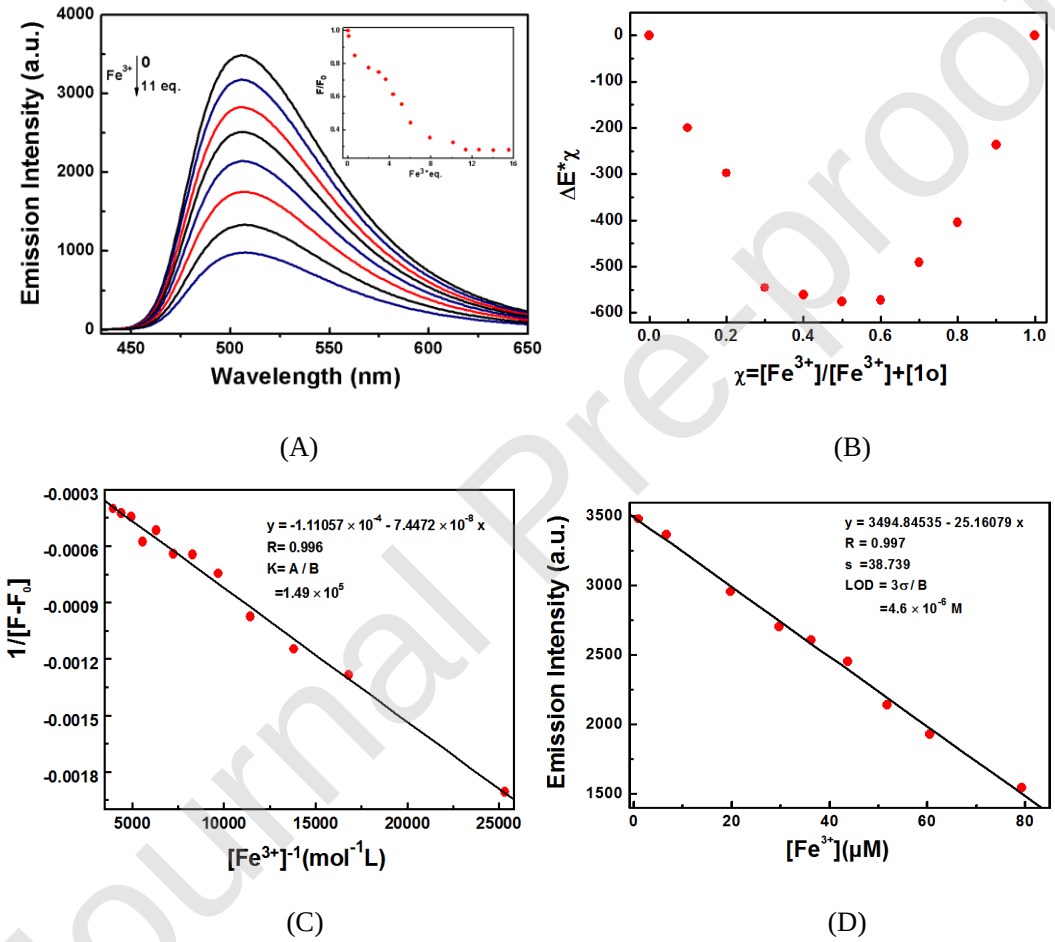

Fig. 4. (A) Fluorescence spectral changes and fluorescence titration of **1o** upon addition of Fe^{3+} (0–11 equiv.) in methanol (1.0×10^{-5} mol L^{-1}), (B) Job's plot showing the 1:1 complex of **1o** with Fe^{3+}, and (C) Hildebrand–Benesi plot based on the 1:1 binding stoichiometry, and (D) The limit of detection (LOD) for Fe^{3+} with **1o**.

Table 1. Comparative study of analytical performance of **1o** with the recently reported sensors for Fe^{3+}.

Structure	Media	Detection limit (mol L^{-1})	Association constant	Approaches	Ref.
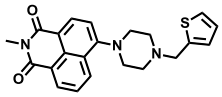	THF/H_2O (6/4, v/v)	3.73×10^{-7}	2.2×10^{4}	Fluorescent	6
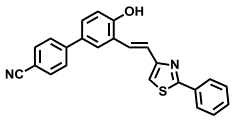	EtOH/H_2O (2/8, v/v)	1.09×10^{-7}	9.8×10^{4}	Fluorescent	4
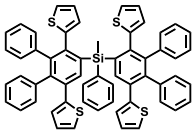	THF/H_2O (6/4, v/v)	1.54×10^{-6}	100	Fluorescent	3
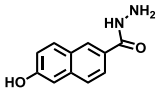	H_2O (pH=7.4)	1.74×10^{-5}	8.8×10^{3}	Fluorescent Colorimetric	33
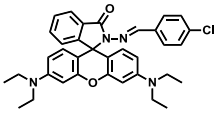	Tris–HCl buffer medium	1.05×10^{-5}	4.0×10^{5}	Fluorescent Colorimetric	5
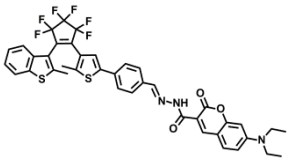	Methanol	4.6×10^{-6}	1.49×10^{5}	Fluorescent	Present work

By adding Fe^{3+}, the emission intensity of **1c** peaked at 506 nm also decreased about 68%, as shown in Fig. 5. The result was consistent with the interaction between Fe^{3+} and **1o**. The closed-ring isomer **1c** had equal capability of recognition of Fe^{3+} compared to the open-ring isomer **1o**. The sensing Fe^{3+} of **1c** was also reversible. Moreover, the complex **1o**–Fe^{3+} showed fluorescence switch changes upon alternating irradiation with UV–vis light, as shown in Fig. S5. The fluorescent modulation efficiency was 66%, which is higher than that of **1o**.

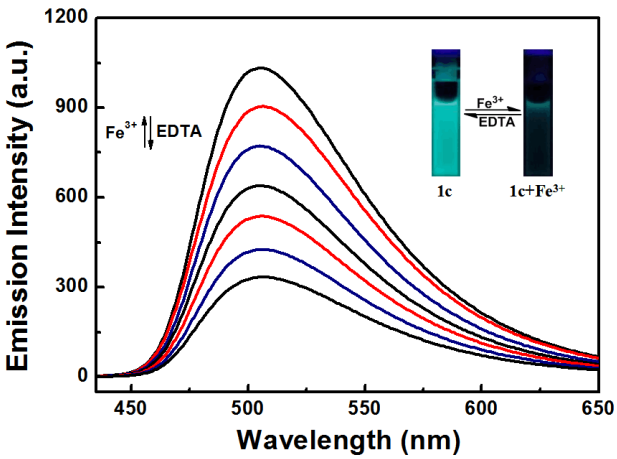

Fig. 5. Fluorescence spectral changes and color changes of **1c** in methanol (1.0×10^{-5} mol L^{-1}) in the presence of Fe^{3+}.

3.3 pH studies

The dependence of emission intensity of the **1o** and its Fe^{3+} complex on the pH of the mediun were studied in the pH range of 3.0–11.0 at **1o** (1.0×10^{-5} mol^{-1} L), Fe^{3+} in methanol. As shown in Fig. 6, the emission intensities of **1o** were high and remained almost constant in the pH range of 3.0–11.0. After mixing **1o** with Fe^{3+}, the emission intensity decreased at all pH values, and remained constant in the range of 3.0–11.0. These data showed that **1o** can be used to detect Fe^{3+} in a wide range of pH including at physiological pH.

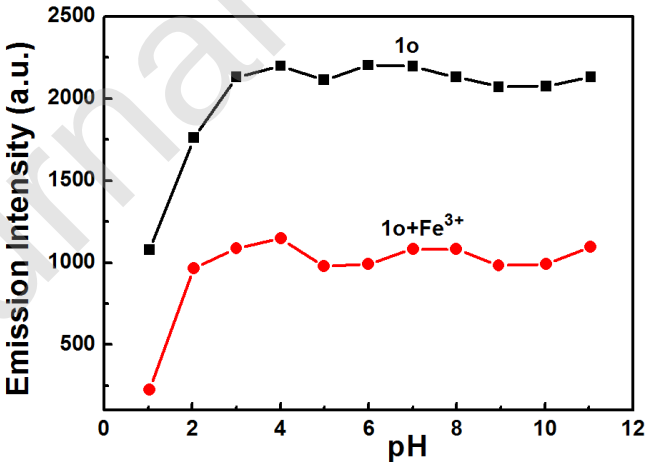

Fig. 6. Fluorescence emission intensity of **1o** in methanol solution *vs* pH before and after addition of 11 equiv. Fe^{3+}. The pH of the solutions was adjusted by addition of 0.1 mol L^{-1} HCl (or 0.1 mol L^{-1} NaOH).

3.4 Possible binding mechanism of **1o** to Fe^{3+}

To gain a clear understanding of the possible binding mode of **1o** with Fe^{3+} , the low resolution mass spectrometry (LRMS) and FT-IR analysis were employed. The peak at m/z 981.0 was assignable to [**1o** + Fe^{3+} + 2 NO_3^- + Na – H]$^+$ (m/z calcd: 981.1), that verified the complex formation. As shown in Fig. S6, a band at around 3058 cm^{-1} could be assigned to the –NH group of hydrazide group. In the complex spectrum, the peak disappeared which indicated that the hydrazide involved the complexation. At the same time, the band at around 2696 cm^{-1} decreased and the peak at 1513 cm^{-1} became narrower. The band of Schiff base (C=N) appeared as a single band at 1617 cm^{-1} in the spectrum of **1o**, which was not affected by adding Fe^{3+}. Moreover, the band showed a clear distinction at 1385 cm^{-1} after addition of Fe^{3+} suggesting the participation of carbonyl of the lactone (C=O) group. These observations revealed that Fe^{3+} binding with **1o** was mainly through the nitrogen at the imine moiety and the oxygen atom at the carbonyl of the lactone (C=O) group. The possible structure of the **1o**-complex was shown in Scheme 1.

3.5 Practical Application

3.5.1 Fluorimetric test paper strip measurement

To investigate the practical application of the fluorimetric sensor, test strips measurement were conducted. First, the Whatman filter papers were immersed into the methanol solution of **1o** (0.001 mol L^{-1}), then drying them at room temperature [41,42]. As shown in Fig. 7A, the fluorescence color change of test strips soaked with **1o** from green to cyan was immediately observed after dropwise addition of Fe^{3+}, wherease, other interfering metal ions (Cr^{3+}, Mn^{2+}, Co^{2+}, Ni^{2+}, Cu^{2+}, Zn^{2+}, Cd^{2+}, Hg^{2+}, Pb^{2+}, K^+, Mg^{2+}, Ca^{2+}, Ba^{2+}, Sn^{2+} and Al^{3+}) did not produce an obvious fluorescence color change.

Therefore, **1o** would be very useful for the fabrication of sensing devices with fast and convenient detection of Fe^{3+} ions. On the other hand, with the increase of Fe^{3+}, the fluorescence color of test strips soaked with **1o** changed from green to indigo even in the presence of 1.0×10^{-4} mol L^{-1} of Fe^{3+}, as shown in Fig. 7B. The minimal concentration of Fe^{3+} detectable of the **1o** test papers was 1.0×10^{-4} mol L^{-1}.

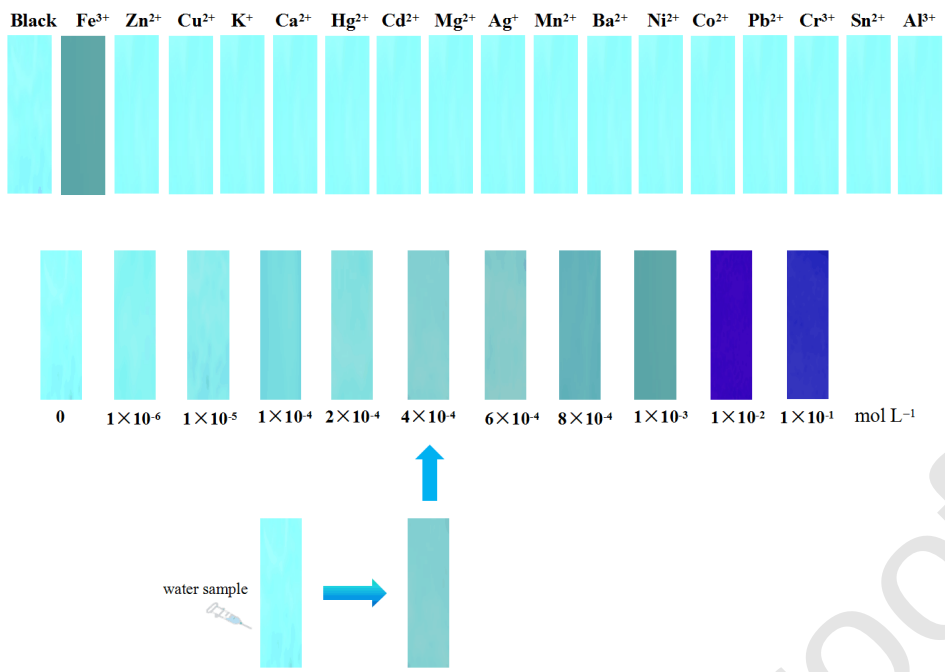

Fig. 7. (A) Photographs of test strips for detecting various anions including Cr^{3+}, Fe^{3+}, Mn^{2+}, Co^{2+}, Ni^{2+}, Cu^{2+}, Zn^{2+}, Cd^{2+}, Hg^{2+}, Pb^{2+}, K^{+}, Mg^{2+}, Ca^{2+}, Ba^{2+}, Sn^{2+} and Al^{3+} in methanol (1.0×10^{-3} mol L^{-1}), and (B) Standard card for Fe^{3+} concentration detection in an wastewater sample.

3.5.2 Practical application to water samples

As a fluorescent sensor, **1o** was further studied for determination of Fe^{3+} in tap water and the Ganjiang river water by standard addition method [43]. Both the water samples were filtered three times through a 0.2 mm membrane filter, then were spiked with a given amount of Fe^{3+}, and finally analyzed by using familiar procedures. As shown in Table 2, the recovery for Fe^{3+} was from 92.7 to over 105.5 %. Therefore, **1o** can be used to detect the spiked Fe^{3+} with the satisfactory recovery.

Table 2. Detection of Fe^{3+} in environmental water samples.

Tap water			Ganjiang River		
Spiked (μmol L^{-1})	Recovered (μmol L^{-1})	Recovery (%)	Spiked (μmol L^{-1})	Recovered (μmol L^{-1})	Recovery (%)
9.0	9.49	105.45	9.0	8.83	98.15
11.0	10.20	92.75	11.0	11.02	100.21
13.0	12.87	98.98	13.0	13.51	103.89

15.0	14.51	96.73	15.0	13.81	92.09

4. Conclusion

A diarylethene derivative containing a photochromic core and an acylhydrazone Schiff base moiety was successfully synthesized, which provided a photochromic FRET system. The compound exhibits the fluorescence from the coumarin-3-hydrazide-1-benzaldehyde Schiff base, which was readily modulated upon alternative irradiation with UV and visible lights. On the other hand, a strong fluorescence quenching was observed upon addition of Fe^{3+}. A pH titration showed that **1o** had stable fluorescence property over a wide pH range of 3.0–11.0, which suggests that **1o** is suitable for application under physiological conditions. Moreover, the fluorimetric test paper strips soaked with **1o** was prepared which could showed highly selective for sensing Fe^{3+}. Based on the standard card, the Fe^{3+} in water samples can be detected conveniently.

We declare that we do not have any commercial or associative interest that represents a conflict of interest in connection with the work submitted. The manuscript entitled “A diarylethene derived Fe^{3+} fluorescent chemosensor and its application in wastewater analysis”.

We declare that we do not have any commercial or associative interest that represents a conflict of interest in connection with the work submitted.

Acknowledgments

The authors are grateful for the financial support from the National Natural Science Foundation of China (41867053), the “5511” science and technology innovation talent project of Jiangxi (2016BCB18015), the key project of Natural Science Foundation of Jiangxi Province (20171ACB20025), the Project of Jiangxi Science and Technology Normal University Advantage Sci-Tech Innovative Team (2015CXTD002), the Project of the Science Funds of Jiangxi Education Office (GJJ180621), and the Open Project Program of “311 high level engineering center”, Jiangxi Science and Technology Normal University (KFGJ18004).

Appendix

For **Fig. S1** to **Fig. S9**, please refer to supplementary information.

References

[1] B. Niu, K. Xiao, X. Huang, Z. Zhang, X.Y. Kong, Z.Q. Wang, L.P. Wen, L. Jiang. High-sensitivity detection of iron (III) by dopamine-modified funnel-shaped nanochannels. ACS Appl Mater Inter. 10 (2018) 22632–22639.

[2] S.J. Dixon, B.R. Stockwell. The role of iron and reactive oxygen species in cell death. Nat Chem Biol. 10 (2014) 9–17.

[3] X. Wang, H. Wang, S. Feng. A novel thiophene functionalized silicon-cored compounds: aggregation-induced emission enhancement and aqueous fluorogenic Fe^{3+} probes in bovine serum albumin. Sens Actuators B. 241 (2017) 65–72.

[4] X. Tang, Y. Wang, J. Han, L. Ni, L. Wang, L.H. Li, H.Q. Zhang, C. Li, J. Li, H.R. Li. A relay identification fluorescence probe for Fe^{3+} and phosphate anion and its applications. Spectrochim Acta A. 191 (2018) 172–179.

[5] P.S. Nayab, M. Shkir. Rapid and simultaneous detection of Cr (III) and Fe (III) ions by a new naked eye and fluorescent probe and its application in real samples. Sens Actuators B. 251 (2017) 951–957.

[6] S.K. Dwivedi, R.C. Gupta, R. Ali, S.S. Razi, S.K. Hira, P.P. Manna, A. Misra. Smart PET based organic scaffold exhibiting bright“turn–on” green fluorescence to detect Fe^{3+} ion: live cell imaging and logic implication. J Photoch Photobio A. 358 (2018) 157–166.

[7] L.C. Foong, M.U. Imam, M. Ismail. Iron-binding capacity of defatted rice bran hydrolysate and bioavailability of iron in Caco-2 cells. J Agr Food Chem J. 63 (2015) 9029–9036.

[8] G.Y. Gao, W.J. Qu, B.B. Shi, Q. Lin, H. Yao, Y.M. zhang, J. Chang, Y. Cai, T.B. wei. A reversible fluorescent chemosensor for iron ions based on 1H-imidazo [4,5-b] phenazine derivative. Sens Actuators B. 213 (2015) 501–507.

[9] S.A. Lee, G.R. You, Y.W. Choi, H.Y. Jo, A.R. Kim, I. Noh, S.J. Kim, Y.M. Kim, C. Kim. A new multifunctional Schiff base as a fluorescence sensor for Al^{3+} and a colorimetric sensor for CN^{-} in aqueous media: an application to bioimaging. Dalton T. 43 (2014) 6650–6659.

[10] A. Saravanan, S. Shyamsivappan, T. Suresh, G. Subashini, K. Kadirvelu, N. Bhuvanesh, R. Nandhakumar, P.S. Mohan. An efficient new dual fluorescent pyrene based chemosensor for the detection of bismuth (III) and aluminium (III) ions and its applications in bio-imaging. Talanta. 198 (2019) 249–256.

[11] Y.H. Yan, H.L. Ma, J.Y. Miao, B.X. Zhao, Z.M. Lin. A ratiometric fluorescence probe based on a novel recognition mechanism for monitoring endogenous hypochlorite in living cells. Anal Chim Acta. 1064 (2019) 87–93.

[12] P.G. Rao, B. Saritha, T.S. Rao. Highly selective reaction based colorimetric and fluorometric chemosensors for cyanide detection via ICT off in aqueous solution. J Photoch Photobio A. 372 (2019) 177–185.

[13] M. Morimoto, Y. Takagi, K. Hioki, T. Nagasaka, H. Sotome, S. Ito, H. Miyasaka, M. Irie. A turn-on mode fluorescent diarylethene: solvatochromism of fluorescence. Dyes Pigments. 153 (2018) 144–149.

[14] G.R. Zou, C.X. Liu, C. Cong, Z.T. Fang, W. Yang, X.M. Luo, S.K. Jia, F. Wu, X. Zhou. 5-Formyluracil as a cornerstone for aluminum detection in vitro and in vivo: a more natural and sustainable strategy. Chem Commun. 54 (2018) 13107–13110.

[15] S.Z. Pu, Q. Sun, C.B. Fan, R.J. Wang, G. Liu. Recent advances in diarylethene-based multi-responsive molecular switches. J Mater Chem C. 4 (2016) 3075–3093.

[16] R. Kashihara, M. Morimoto, S. Ito, H. Miyasaka, M. Irie. Fluorescence photoswitching of a diarylethene by irradiation with single-wavelength visible light. J Am Chem Soc. 139 (2017) 16498–16501.

[17] I Tchikawa, M Morimoto, M Irie. Diastereoselective photocyclization of a photochromic diarylethene having a benzo [b] phosphole P-oxide group. Dyes Pigments. 137 (2017) 214–220.

[18] K. Uno, M.L. Bossi, M. Irie, V.N. Belov, S.W. Hell. Reversibly photoswitchable fluorescent diarylethenes resistant against photobleaching in aqueous solutions. J Am Chem Soc. 141 (2019) 16471–16478.

[19] C.M. Davis, E.S. Childress, E.J. Harbron. Ensemble and single-particle fluorescence photomodulation in diarylethene-doped conjugated polymer nanoparticles. J Phys Chem C. 115 (2011) 19065–19073.

[20] B. Roubinet, M. Weber, H. Shojaei, M. Bates, M. L. Bossi, V. N. Belov, M. Irie, S. W. Hell. Fluorescent photoswitchable diarylethenes for biolabeling and single-molecule localization microscopies with optical superresolution. J Am Chem Soc. 139 (2017): 6611–6620.

[21] H.Q. Li, L. Cai, Z. Chen. Coumarin-derived fluorescent chemosensors. Advances in chemical sensors. 6 (2012) 121–150.

[22] X.H. Qian, Y. Xiao, Y.F. Xu, X.F. Guo, J.H. Qian, W.P. Zhu. "Alive" dyes as fluorescent sensors: fluorophore, mechanism, receptor and images in living cells. Chem Commun. 46 (2010) 6418–6436.

[23] Y.X. Chang, J.X. Fu, K. Yao, K.X. Xu, X.B. Pang. Novel fluorescent probes for sequential detection of Cu^{2+} and citrate anion and application in living cell imaging. Dyes Pigments, 161 (2019) 331–340.

[24] R. Kaur, J.S. Sidhu, N. Singh, I. Kaur, N. Kaur. Cystamine-cobalt complex based fluorescent sensor for detection of NADH and cancer cell imaging. Sens Actuators B. 293 (2019) 144–150.

[25] Z.G. Gao, C. Kan, H.B. Liu, J. Zhu, X.F. Bao. A highly sensitive and selective fluorescent probe for Fe^{3+} containing two rhodamine B and thiocarbonyl moieties and its application to live cell imaging. Tetrahedron, 75 (2019) 1223–1230.

[26] M.E. Shirbhate, Y. Jeong, G. Ko, G. Baek, G. Kim, Y.U. Kwon, K.M. Kim, J. Yoon. Selective fluorescent recognition of Zn^{2+} by using chiral binaphthol-pyrene probes. Dyes Pigments, 167 (2019) 29–35.

[27] H.L. Liu, S.Q. Cui, F. Shi, S.Z. Pu. A diarylethene based multi-functional sensor for fluorescent detection of Cd^{2+} and colorimetric detection of Cu^{2+}. Dyes Pigments. 161 (2019) 34–43.

[28] D.D. Xue, C.H. Zheng, S.Z. Qu, G.M. Liao, C.B. Fan, G. liu, S.Z. Pu. A highly selective fluorescent chemosensor for Cu^{2+}: synthesis and properties of a rhodamine B-containing diarylethene. Luminescence. 32 (2017) 652–660.

[29] H.C. Ding, B.Q. Li, S.Z. Pu, G. liu, D.C. Jia, Y. Zhou. A fluorescent sensor based on a diarylethene-rhodamine derivative for sequentially detecting Cu^{2+} and arginine and its application in keypad lock. Sens Actuators B. 247 (2017) 26–35.

[30] S.H. Jing, C.H. Zheng, S.Z. Pu, C.B. Fan, G. Liu. A highly selective ratiometric fluorescent chemosensor for Hg^{2+} based on a new diarylethene with a stilbene-linked terpyridine unit. Dyes Pigments. 107 (2014) 38–44.

[31] T.T. Zhang, C.H. Zheng, S.Z. Qu, G. Liu, S.Z. Pu. Modulating the selectivity of a colorimetric sensor based on a Schiff base-functionalized diarylethene towards anions by judicious choice of solvent. J Photoch Photobio A. 375 (2019) 9–17.

[32] S.Z. Pu, L.L. Ma, G. Liu, H.C. Ding, B. Chen. A multiple switching diarylethene with a phenyl-linked rhodamine B unit and its application as chemosensor for Cu^{2+}. Dyes Pigments. 113 (2015) 70–77.

[33] N.N. Li, Y.Q. Ma, X.J. Sun, M.Q. Li, S. Zeng, Z.Y. Xing, J.L. Li. A dual-function probe based on naphthalene for fluorescent turn-on recognition of Cu^{2+} and colorimetric detection of Fe^{3+} in neat H_2O. Spectrochimica Acta A. 210 (2019) 266–274.

[34] T. Nakashima, K. Miyamura, T. Sakai, T. Kawai. Photo-, solvent-, and ion-controlled multichromism of imidazolium-substituted diarylethenes. Chem-Eur J. 15 (2009) 1977–1984.

[35] F.A. Bennett, D.J. Barlow, A.N.O. Dodoo, R.C. Hider, A.B. Lansley, M.J. Lawrence, C. Marriott, S.S. Bensal. L-(6, 7-dimethoxy-4-coumaryl) alanine: an intrinsic probe for the labelling of peptides. Tetrahedron Lett. 38 (1997) 7449–7452.

[36] S.H. Gellman, G.P. Dado, G.B. Liang, B.R. Adams. Conformation-directing effects of a single intramolecular amide-amide hydrogen bond: variable-temperature NMR and IR studies on a homologous diamide series. J Am Chem Soc. 113 (1991) 1164–1173.

[37] D. Kim, J.E. Kwon, S.Y. Park. Fully reversible multistate fluorescence switching: organogel system consisting of luminescent cyanostilbene and turn-on diarylethene. Adv Funct Mater. 28 (2018) 1706213.

[38] L. Giordano, T.M. Jovin, M. Irie, E.A. Jares-Erijman. Diheteroarylethenes as thermally stable photoswitchable acceptors in photochromic fluorescence resonance energy transfer (pcFRET). J Am Chem Soc. 124 (2002) 7481–7489.

[39] S. Warrier, P.S. Kharkar. Highly selective on-off fluorescence recognition of Fe^{3+} based on a coumarin derivative and its application in live-cell imaging. Spectrochimica Acta A. 188 (2018) 659–665.

[40] H.S. Jung, P.S. Kwon, J.W. Lee, J.Il. Kim, C.S. Hong, J.W. Kim, S.H. Yan, J.Y. Lee, J.H. Lee, T. Joo, J.S. Kim. Coumarin-derived Cu^{2+}-selective fluorescence sensor: synthesis, mechanisms, and applications in living cells. J Am Chem Soc. 131 (2009) 2008–2012.

[41] X.Y. Kong, L.J. Hou, X.Q. Shao, S.M. Shuang, Y. Wang, C. Dong. A phenolphthalein-based fluorescent probe for the sequential sensing of Al^{3+} and F^{-} ions in aqueous medium and live cells. Spectrochim Acta A. 208 (2019) 131–139.

[42] Y.X. Zhuge, D.M. Xu, C.H. Zheng, S.Z. Pu. An ionic liquid-modified diarylethene: Synthesis, properties and sensing cyanide ions. Anal Chim Acta. 1014 (2019) 153–163.

[43] W.C. Lin, J.W. Hu, K.Y. Chen. A ratiometric chemodosimeter for highly selective naked-eye and fluorogenic detection of cyanide. Anal Chim Acta. 893 (2015) 91–100.